# FEM-based Subdivision Solids for Dynamic and Haptic Interaction

**Kevin T. McDonnell** **Hong Qin**

Department of Computer Science
State University of New York at Stony Brook
Stony Brook, NY 11794-4400
{ktm|qin}@cs.sunysb.edu

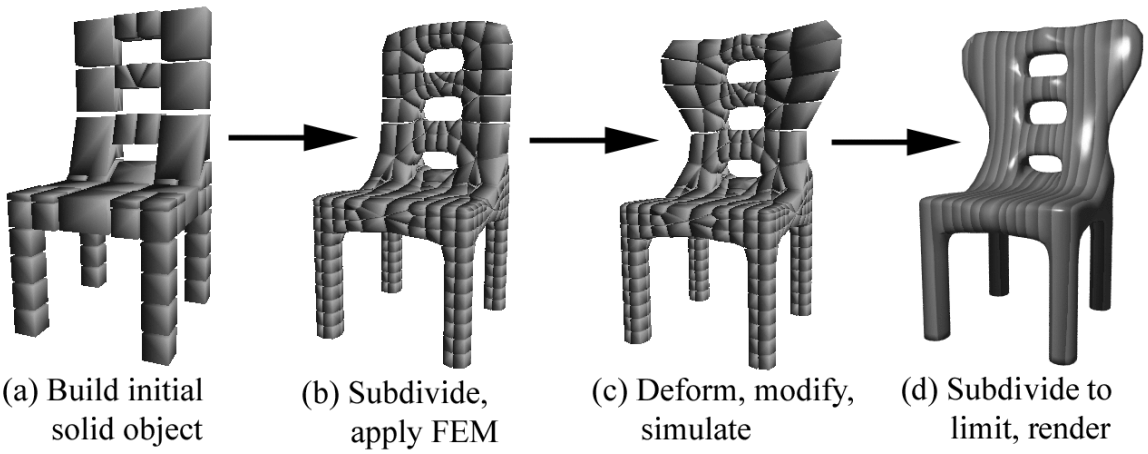


Figure 1: The design, manipulation and simulation processes featured in our novel dynamic solid modeling approach.

## 1 Introduction and Contribution

In this research we systematically formulate a novel physics-based solid model that can overcome many of the limitations associated with conventional solid modeling techniques. Within our new dynamic modeling framework, free-form subdivision solids [2] are equipped with continuous mass and stiffness distributions, internal deformation energies, and other material and graphical properties such as color and density. In contrast with mature modeling techniques associated with subdivision surfaces, our solid formulations based on subdivision transcend surface-based approaches by defining geometry and topology both in the interior and on the boundary of solid objects. We have implemented a prototype design environment based on dynamic subdivision solids in which users can interact with virtual objects via forces and simulate and analyze their dynamic behavior either at run-time (for simple models) or offline (for complex models).

## 2 FEM-based Subdivision Solids

### 2.1 Overview

In our FEM-based subdivision solids, each cell in the subdivided solid is treated as a polyhedral finite element that has a continuous material distribution throughout the cell. For example, the chair model in Figure 1(b) shows the individual elements that comprise the piece of furniture. Material distributions are defined continuously throughout the entire solid space and can be modified anywhere by the user.

Like many subdivision surface algorithms, the subdivision solid algorithm can be expressed as a global matrix multiplication:

$$\mathbf{d} = \mathbf{A}\mathbf{p}, \tag{1}$$

where $\mathbf{p}$ is a vector consisting of the components of the control points; the matrix $\mathbf{A}$ is a sparse matrix whose entries are determined by the subdivision rules; and the vector $\mathbf{d}$ concatenates all the components of the nodal points that are used to approximate the limit solid after a certain number of subdivisions.

### 2.2 Dynamic Formulation

Our dynamic formulation starts from the following discrete form of the Lagrangian equation of motion :

$$\mathbf{M}\ddot{\mathbf{x}} + \mathbf{D}\dot{\mathbf{x}} + \mathbf{K}\delta_{\mathbf{x}} = \mathbf{f}_{\mathbf{x}} \tag{2}$$

The $\mathbf{M}$, $\mathbf{D}$ and $\mathbf{K}$ matrices represent the mass, damping and internal energy distributions, respectively, of a modeled object. Note that, $\dot{\mathbf{x}}$ and $\ddot{\mathbf{x}}$ are the velocity and acceleration of the discretized

object $\mathbf{x}$, respectively. The $\delta_{\mathbf{x}}$ is the companion displacement vector derived from $\mathbf{x}$. For small deformations, we can approximate $\delta_{\mathbf{x}}$ using $\mathbf{x} - \mathbf{x}_0$, where the subscript denotes the rest shape. For large deformations, however, $\delta_{\mathbf{x}}$ may take on various application-dependent forms. The $\mathbf{f_x}$ collects the total external forces acting on $\mathbf{x}$.

We associate with the FEM equation of motion geometric and topological quantities of a subdivision solid. Below, the vector $\mathbf{f_d}$ denotes the external forces acting on each nodal point. The physics of the subdivision solid is subject to the constraints defined by Equation 1:

$$\mathbf{M}\ddot{\mathbf{d}} + \mathbf{D}\dot{\mathbf{d}} + \mathbf{K}\delta_{\mathbf{d}} = \mathbf{f_d},$$

where, in general, the deformation can be characterized by $\delta_{\mathbf{d}} = \mathbf{Bd} + \mathbf{Cd}_0$, which is amenable to both large and small deformations. Note that, two linear matrix operators $\mathbf{B}$ ($\mathbf{B}$ is also symmetric) and $\mathbf{C}$ approximate *higher-order* variations such as stretching and bending and *lower-order* variations such as displacement, respectively. This decomposition results in a much simpler formulation for $\mathbf{K}$ that is no longer a function of $\mathbf{d}$. This has the desired effect of greatly improving the time performance of our subdivision solids. Let us further investigate the FEM equation:

$$\mathbf{A}^\top\mathbf{M}\ddot{\mathbf{d}} + \mathbf{A}^\top\mathbf{D}\dot{\mathbf{d}} + \mathbf{A}^\top\mathbf{KBd} = \mathbf{A}^\top\mathbf{f_d} - \mathbf{A}^\top\mathbf{KCd_0}$$

$$\mathbf{A}^\top\mathbf{MA}\ddot{\mathbf{p}} + \mathbf{A}^\top\mathbf{DA}\dot{\mathbf{p}} + \mathbf{A}^\top\mathbf{KBAp} = \mathbf{A}^\top\mathbf{f_d} - \mathbf{A}^\top\mathbf{KCAp_0} \tag{3}$$

Using the FEM procedure and the discretized approximation of continuous dynamic solids, we compute local element matrices and iteratively evolve the time integration.

### 2.3 Discrete Dynamics Equations

Equation 3 is integrated numerically through time using an implicit solver as follows. Discrete derivatives are computed using backward differences: $\ddot{\mathbf{p}}_{i+1} = (\mathbf{p}_{i+1} - 2\mathbf{p}_i + \mathbf{p}_{i-1})/(\Delta t^2)$, $\dot{\mathbf{p}}_{i+1} = (\mathbf{p}_{i+1} - \mathbf{p}_{i-1})/(2\Delta t)$. We derive the time integration formula

$$\left(2\mathbf{M_p} + \Delta t\mathbf{D_p} + 2\Delta t^2\mathbf{K_p}\right)\mathbf{p}_{i+1} = 2\Delta t^2\mathbf{f_p} + 4\mathbf{M_p}\mathbf{p}_i - (2\mathbf{M_p} - \Delta t\mathbf{D_p})\mathbf{p}_{i-1}, \tag{4}$$

where $\mathbf{M_p} = \mathbf{A}^\top\mathbf{MA}$, $\mathbf{D_p} = \mathbf{A}^\top\mathbf{DA}$, $\mathbf{K_p} = \mathbf{A}^\top\mathbf{KBA}$, $\mathbf{f_p} = \mathbf{A}^\top\mathbf{f_d} - \mathbf{A}^\top\mathbf{KCAp_0}$ and the subscripts denote evaluation of the quantities at the indicated time-steps.

It is straightforward to employ the conjugate gradient method [3] to obtain an iterative solution for $\mathbf{p}_{i+1}$. The number of conjugate gradient iterations per time-step can be increased to improve the accuracy of the solver, but at the expense of efficiency.

### 2.4 Hexahedral Cells

After several subdivisions on the initial control lattice, the vast majority of cells in the subdivided lattice are hexahedra. We assign one finite element to each such cell that appears in the subdivided lattice. Each element consists of the eight vertices that comprise the cell geometry and characterize the FEM shape functions. Shape functions are used to define the continuous material distributions across the cells. Since a MacCracken-Joy subdivision solid has no global parameterization, each element is parameterized independently of the other elements. We associate a tri-linear, eight-node hexahedral element with each regular cell because of its convenience and generality. The shape functions can be integrated using Gaussian quadrature [3] and stored in the row vector $\mathbf{J}$ as follows:

$$\mathbf{J} = [B_0 \quad B_1 \quad \cdots \quad B_7]$$

The mass, damping and stiffness distributions are then computed as follows. Let $\mu(u, v, w)$ and $\gamma(u, v, w)$ be the mass density and damping density functions, respectively, of one element of the solid. Then,

$$\mathbf{M} = \iiint \mu\mathbf{J}^\top\mathbf{J}dudvdw \quad \text{and} \quad \mathbf{D} = \iiint \gamma\mathbf{J}^\top\mathbf{J}dudvdw$$

are $8\times8$ element matrices.

#### 2.4.1 Large and Small Deformations

Our dynamic model supports the realistic simulation of both large and small deformations. The internal energy is separated into stretching and shearing components to characterize an object's resistance to these types of deformation. The corresponding expression for the stiffness matrix $\mathbf{K}$ is

$$\mathbf{K} = \iiint(\alpha\mathbf{J}^\top\mathbf{J})dudvdw + \iiint(\beta\mathbf{J}^\top\mathbf{J})dudvdw$$

where $\alpha(u, v, w)$ and $\beta(u, v, w)$ are the elasticity functions that control local tension and rigidity in the three parametric coordinate directions.

The generalized force vector $\mathbf{f_d}$ can be obtained through the principle of virtual work [1] done by the applied force distribution $\mathbf{f}(u, v, w, t)$ and can be expressed as

$$\mathbf{f_d} = \iiint \mathbf{J}^\top\mathbf{f}(u, v, w, t)dudvdw$$

where $t$ is time.

### 2.5 Special Cells

The presence of high-valence (so-called "extraordinary") vertices in the control lattice results in the creation of non-hexahedral cells in the subdivided solid (used to approximate the continuous solid in the limit). Each of these "special cells" consists entirely of quadrilaterals and has an even number of faces. For these cells we associate a group of quadrilateral surface finite elements with one element per face. The element mass, damping and stiffness matrices are assembled in a similar fashion to those of the normal elements, except that each has only two parametric coordinate directions rather than three.

## 3 Conclusions

We have presented a new, dynamic FEM-based solid modeling framework and have implemented a virtual sculpting system with an intuitive, natural haptic interface based on the novel integration of subdivision solids and physics-based techniques. Future research involving dynamic subdivision solids includes volumetric morphing applications, scientific visualization, physical simulation for flow dynamics and heat transfer, and others.

## References

[1] B. Gossick. *Hamilton's Principle and Physical Systems*. Academic Press, New York, 1967.

[2] R. MacCracken and K. I. Joy. Free-form deformations with lattices of arbitrary topology. In *Computer Graphics (SIGGRAPH 96 Proceedings)*, pages 181–188, August 1996.

[3] W. H. Press, S. A. Teukolsky, W. T. Vetterling, and B. P. Flannery. *Numerical Recipes in C: The Art of Scientific Computing*. Cambridge University Press, Cambridge, second edition, 1992.